Atmospheric Environment 206 (2019) 132–143

Contents lists available at ScienceDirect

Atmospheric Environment

journal homepage: www.elsevier.com/locate/atmosenv

Ozone transport and thermodynamics during the passage of squall line in Central Amazon

Adayana M.Q. Melo[a], Cléo Q. Dias-Junior[b,*], Julia C.P. Cohen[a], Leonardo D.A. Sá[c,1], José Henrique Cattanio[a], Paulo A.F. Kuhn[a]

[a] Institute of Geosciences, Federal University of Pará, Belém, Brazil
[b] Federal Institute of Pará, Department of Physics, Belém, Brazil
[c] Center for Weather Forecasting and Climate Studies, National Institute for Space Research, São José dos Campos, Brazil

ARTICLE INFO

Keywords:
Squall lines
Ozone
Density currents
Low level jets
Amazon rainforest
JULES-CCATT-BRAMS

ABSTRACT

The main objective of this work is to better understand the increase of ozone (O_3) in the surface by the influence of density currents formed by downdrafts from mesoscale convective systems, using as tool the JULES-CCATT-BRAMS model. Initially, the superficial increases of O_3 were investigated with the ECMWF Era-Interim reanalysis that showed a plume rich in O_3 located at middle troposphere along with the increase of this gas' concentration in the surface during the rainy period in Central Amazon. GOES satellite images and surface synoptic charts showed the formation of a squall line (SL) in the interior of the Continent by the influence of a Frontal System that reached the southeast of South America in this period. The numerical simulation results provided an understanding of the three-dimensional structure of the chemistry and thermodynamics of the atmosphere during the passage of this SL at dawn on April 14, 2014. The downdrafts from SL bring cooler, drier, dense air to near the surface. This downdrafts air column passed by the O_3 "plume" in the middle troposphere, formed rich gas density currents and low level jets were induced near the surface and spread the O_3. Finally, this cleaner air column decreased the surface carbon monoxide (CO) levels, and as a result of the increase in O_3 concentration resulted in an increase in surface nitrogen dioxide (NO_2).

1. Introduction

Among the principal atmospheric systems that produce rainfall in the Amazon basin are squall lines (SL) whose origin is associated with the circulation of marine breezes (Kousky, 1980). These SL are formed along the Atlantic coast of the Amazon and frequently propagate into the interior of the continent, having an important role in the distribution of rainfall in the Amazon region (Kousky, 1980; Garstang et al., 1994; Cohen et al., 1995; Alcântara et al., 2011; de Oliveira and Oyama, 2015). Besides breezes SL, another type of SL that forms above the continent was also observed in the southwest portion of the Amazon basin. This SL is frequently associated with a frontal system (FS). They are very rare and propagates from the Southwest to the Northeast of the Amazon basin, generating strong wind gusts known as blowdown winds which cause an increase in tree mortality in the central region of the Amazon (Negrón-Juárez et al., 2010, 2017). Both coast and continental SL consists of cumulonimbus clouds organized linearly that form along the trailing edge of a large downdraft (Houze Jr, 1977). Additionally, low-level jets (LLJ) and the formation of density currents are fundamental mechanisms for the maintenance and propagation of these SL (Alcântara et al., 2014).

Several authors have shown that the presence of SL and their respective downdrafts altered the thermodynamics and chemistry near the surface (Kirchhoff et al., 1990; Betts et al., 2002; Grant et al., 2008; Gerken et al., 2016; Dias-Júnior et al., 2017). Initially it was believed that stratospheric ozone (O_3) is entrained into the thunderstorm at high levels, near or above the tropopause. It is transported into the low levels of the atmosphere by the SL's downdraft (Davis, 1973). More recent investigations (Betts et al., 2002; Grant et al., 2008; Hu et al., 2010; Gerken et al., 2016) indicate that these downdrafts also transport air rich in O_3 from the middle troposphere towards the Earth's surface.

Betts et al. (2002) showed that during the passage of a breeze SL over the State of Rondônia in the western region of the Amazon, O_3 levels abruptly increased during the night, exactly at the moment of the occurrence of downdrafts associated with the SL. They concluded that the passage of the SL was responsible for the decrease in the values of

* Corresponding author.
E-mail address: cleo.quaresma@ifpa.edu.br (C.Q. Dias-Junior).
[1] Retired.

https://doi.org/10.1016/j.atmosenv.2019.02.018
Received 26 June 2018; Received in revised form 10 February 2019; Accepted 12 February 2019
Available online 01 March 2019

the equivalent potential temperature (θ_e) and O_3-enhancement events near the surface. Grant et al. (2008) in rural western Senegal also showed that mesoscale convective systems contributed to diurnal O_3 variations that substantially and abruptly deviated from the diurnal patterns observed during sunny conditions. These deviations were caused by downdrafts of convective storms that carried O_3-rich air from the mid troposphere into the surface, enhancing the boundary layer O_3 levels by 10–30 ppbv. Still according to Grant et al. (2008) the O_3 increases depended on the convective velocities associated with storm downdrafts and origin of the downward moving air parcels.

A particularly interesting question, and one that still requires greater investigation, pertains to the horizontal and vertical dynamics of O_3 during SL occurrences, since a series of other chemical reactions is initiated in the presence of O_3.

Hu et al. (2012) conducted observational experiments and numerical simulations with the Weather Research and Forecasting model with Chemistry (WRF/Chem) in the Beltsville, MD during the summer of 2010. They noticed a significant increase of O_3 on the surface during the day, resulting from pollution events occurring in the city. However, after the beginning of the stable boundary layer (SBL) formation, O_3 levels close to the surface decreased rapidly, whereas in the Residual Layer (RL) levels were still high. These authors also showed that, in the absence of strong disturbances, the dispersion of pollutants between RL and SBL becomes limited. They observed that under conditions of strong turbulence the structure and vertical distribution of pollutants is modified in SBL. Such modification can be triggered by mesoscale movements such as LLJ, gravity waves, Kelvin-Helmholtz instabilities, density currents, wake vortices (Sun et al., 2002, 2004; Salmond and McKendry, 2005). Hu et al. (2013) also using WRF, have confirmed that nocturnal LLJ carry O_3 from RL to near the surface.

Dias-Júnior et al. (2017) observed an increase in the O_3 near the surface caused by downdrafts resulting from the passage of convective systems above the Central Amazon region. The downdrafts induce the emergence of density currents and the subsequent formation of LLJ during the passage of these systems. Dias-Júnior et al. (2017) suggested that the horizontal transport of O_3 near the surface would be due to the presence of these jets; however they lack the experimental data to support their suggestion. Additionally, Alcântara et al. (2014) in their study on the generation and evolution of an Amazon SL identified the existence of LLJ in 87% of the cases of the occurrence of SL. According to the authors, LLJ could be associated with the propagation of these SL over great distances. Interestingly, Alcântara et al. (2014) emphasized the crucial role played by LLJ in the maintenance and propagation of the SL and in the formation of density currents on the trailing edge of this moving system.

A better understanding of what produces O3-accumulation in the lower troposphere (above the forest), associated with mesoscale phenomena (such as SLs), is of great interest when investigating chemical oxidation processes and the formation of aerosols in the tropical troposphere. For example, the Amazon forest emits large quantities of isoprene, monoterpenes, and sesquiterpenes (Guenther et al., 2006; Jardine et al., 2015), and these gases react with free radicals (for example, OH) and are precursors of secondary organic aerosols (Crutzen, 1987; Fuentes et al., 2000; Gerken et al., 2016; Wei et al., 2018).

In order to contribute to our understanding about the role of SL in chemical transport above the Amazon forest we performed a numeric simulation of atmospheric flow during a case study of an O_3-buildup event near the surface generated by a SL above the Amazon forest was reproduced to a highly satisfactory degree. A second main subject of this study was to better understand the horizontal and vertical dynamics of O_3 during the presence of downdrafts originated from the SL.

2. Data and methodology

Data of the precipitation rate estimated by the CMORPH (Climate Prediction Center Morphing Method) (Joyce et al., 2004) and the GOES 13 satellite images in the infrared channel were used to describe the development of SL considered in this work. The CMORPH technique uses the rainfall estimates from Passive Microwave (PMW) sensor onboard polar orbiting satellite exclusively, with infrared data from geostationary satellite to derive a motion field that is used to propagate the rainfall derived by PMW data.

Additionally, the O_3 data and the vertical wind component obtained by ECMWF-Era Interim reanalysis with a 6-h interval and 0.25° spatial resolution were able to evaluate the vertical behavior of these variables during the analyzed period.

The numeric simulation was conducted using the mesoscale model BRAMS (Brazilian Regional Atmospheric Modeling System) version 5.3. This version is composed of the coupling of the models JULES (Joint UK Land Environment Simulator) (Best et al., 2011; Clark et al., 2011) and CCATT (Coupled Chemistry-Aerosol-Tracer Transport) (Freitas et al., 2009), therefore making BRAMS a new numeric system of modeling of atmosphere-biosphere-chemistry interactions that is totally coupled and is called the JULES-CCATT-BRAMS model (Moreira et al., 2013; Freitas et al., 2017a).

This study used the JULES-CCATT-BRAMS model in order to perform numerical simulations that permit a greater understanding of the influence of a SL (formed on April 14, 2014) upon the thermodynamics and chemistry of the atmosphere above Amazon. The SL's occurrence is noticeable in satellite images and its presence caused several changes which were observed on the regional thermodynamic data and in the O_3-levels near the surface, as will be shown in the Results section. A numeric experiment was conducted that had an integration time of 36h, and was started at 12 UTC on April 13 and continued until 00 UTC on April 15, 2014, with output every 10 min.

The simulation was performed using a grid with a horizontal resolution of 8 km with 135 points in the x and y dimensions, and 35 points in the z dimension. The vertical resolution of the grid was variable with an initial vertical spacing of 90 m that increased by a factor of 1.1 up to 1 km, and from this point onward the spacing was maintained constant up to the top of the model at approximately 18 km. The choice of this domain and horizontal resolution for this grid were determined in function of the extension of the SL and also the computational capacity available for the execution of the numeric simulation. The domain covered by this grid, the distribution of the principal rivers, and the surface topography are shown in Fig. 1. The dominant

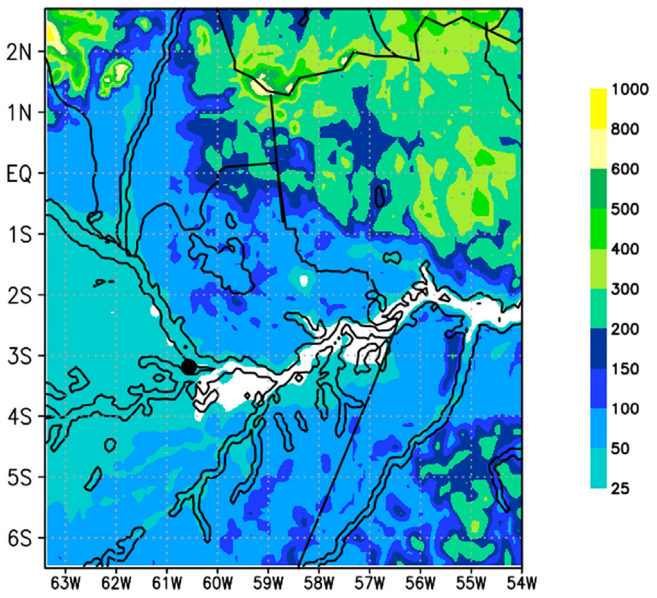

Fig. 1. Simulation domain with topography (meters, shading) and large rivers distribution. The black circle represents Manacapuru (3.21° S 60.60° W) research site.

vegetation type in this domain is forest with small areas of pasture (not shown).

The initialization of the model was heterogeneous, with ECMWF's Era Interim Re-Analysis datasets, made available by CPTEC-INPE in each 6-h interval and with spatial resolution of 0.25°. Seven soil layers were defined up to a depth of 12.25 m, and soil humidity was assumed to be heterogeneous, as described by Freitas (2006). Soil texture data were originally obtained from the Food and Agriculture Organization of the United Nations (UNFAO) and were adapted for the Brazilian territory by INPE (Rossato et al., 2004).

In this simulation the Grell-Freitas deep cumulus parametrizations (Grell and Freitas, 2014) and Grell-Devenyi's shallow (Grell and Dévényi, 2002) were used. Grell-Devenyi's shallow cumulus parametrization was included in JULES-CCATT-BRAMS, mainly due to the necessity of a convective trace gas transport consistent mass flow scheme (Freitas et al., 2017b). Grell-Devenyi expanded the original parameterization of Grell (1993), and included the ability to use a large number of set members based on five different types of closed formulations (ENSEMBLE), resulting in a higher precipitation efficiency and the capacity of the air parcels to overcome the convective inhibition energy (Freitas et al., 2017a).

The Grell-Freitas scheme (Grell and Freitas, 2013) for the parametrization of the deep cumulus is based on the original Grell-Devenyi approach (Grell and Dévényi, 2002), with the use of scale dependence formulations for high-resolution simulations (or “gray-zone” for deep convection models configuration) and the interaction with aerosols.

The cloud microphysics using Greg Thompson's formulation of “single moment in cloud liquid water” was also used (Thompson et al., 2008; Thompson and Eidhammer, 2014), which consists in the separate treatment of five classes of water that, later on, are mixed in a single-moment treatment for each type of cloud, thus optimizing computational time. In addition, it includes the activation of aerosols in the condensation of cloud nuclei (CCN) and ice (IN), in this way, it predicts the concentration of the number of water droplets in the clouds, as well as the concentrations of two new aerosol variables, one for CCN and one for IN, these variables are grouped into two different groups according to their hygroscopicity: hygroscopic aerosols are called “water friendly” and non-hygroscopic aerosols are the “ice friendly” (Freitas et al., 2017a).

The parameterization used for long and short wave radiation was from CARMA (Community Aerosol and Radiation Model for Atmospheres) (Rosário et al., 2013), which resolves the radiative transfer using the method of two-fluxes and includes the principal molecular absorption species (water vapor, CO, O_3 and O_2). Additionally, the coefficients of gas absorption were included (Toon et al., 1989) and radiation schemes of JULES-CCATT-BRAMS are coupled online with microphysical models of clouds and aerosols in order to provide online simulations of aerosol-cloud-radiation interactions (Freitas et al., 2017a). The physical and optical properties of clouds in the CARMA radiation scheme were parameterized according to Sun and Shine (1994) using profiles of liquid water and ice content provided by the model of the microphysics of clouds of the JULES-CCATT-BRAMS model (Freitas et al., 2017a).

3. Results and discussion

The motivation for the accomplishment of this work was due to the presence of a “plume” of O_3 (reanalysis data from the ECMWF Era-Interim dataset) in the middle troposphere, during April 10–14, 2014, exactly on the days in which O_3-buildup events were observed near the surface at the experimental site of Manacapuru (Fig. 1) during the GoAmazon project (Observations and Modeling of the Green Ocean Amazon) (Martin et al., 2016). It was observed that the superficial levels of O_3 only increased significantly (above 10 ppbv) when the downdraft pass by the O_3 plume occurred. This aspect will be analyzed in detail in the next sections with help of JULLES-CCATT-BRAMS

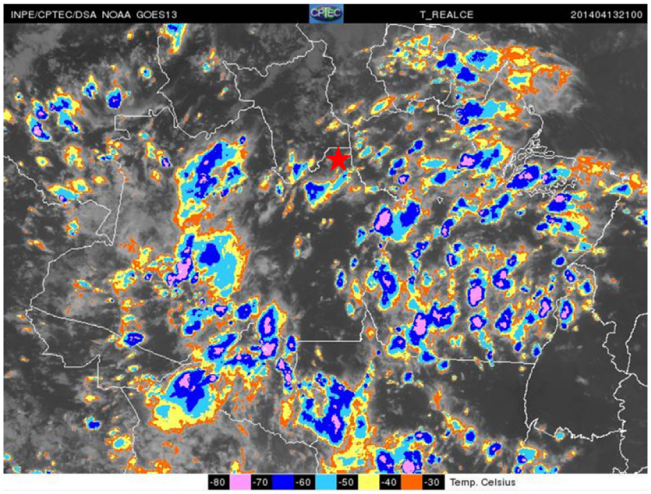

(a)

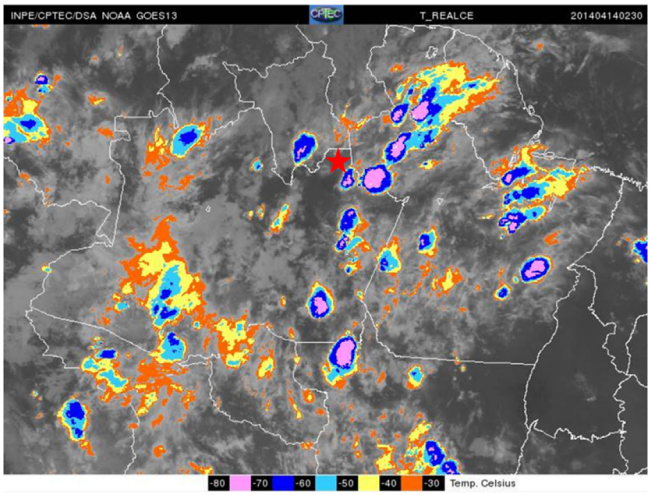

(b)

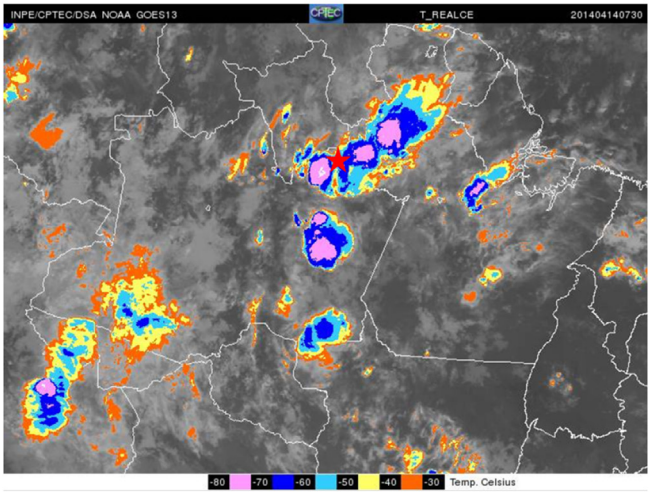

(c)

Fig. 2. Satellite images from GOES-13 on the infrared channel, showing the different stages of two SL that passed over the Manacapuru site on April 14, 2014. (a) 21 UTC (April 13), (b) 0230 UTC (April 14) and (c) 0730 UTC (April 14). The red star indicates the region of greatest system precipitation rate (0.70° *S* 59.10° *W*), discussed later. (For interpretation of the references to color in this figure legend, the reader is referred to the Web version of this article.)

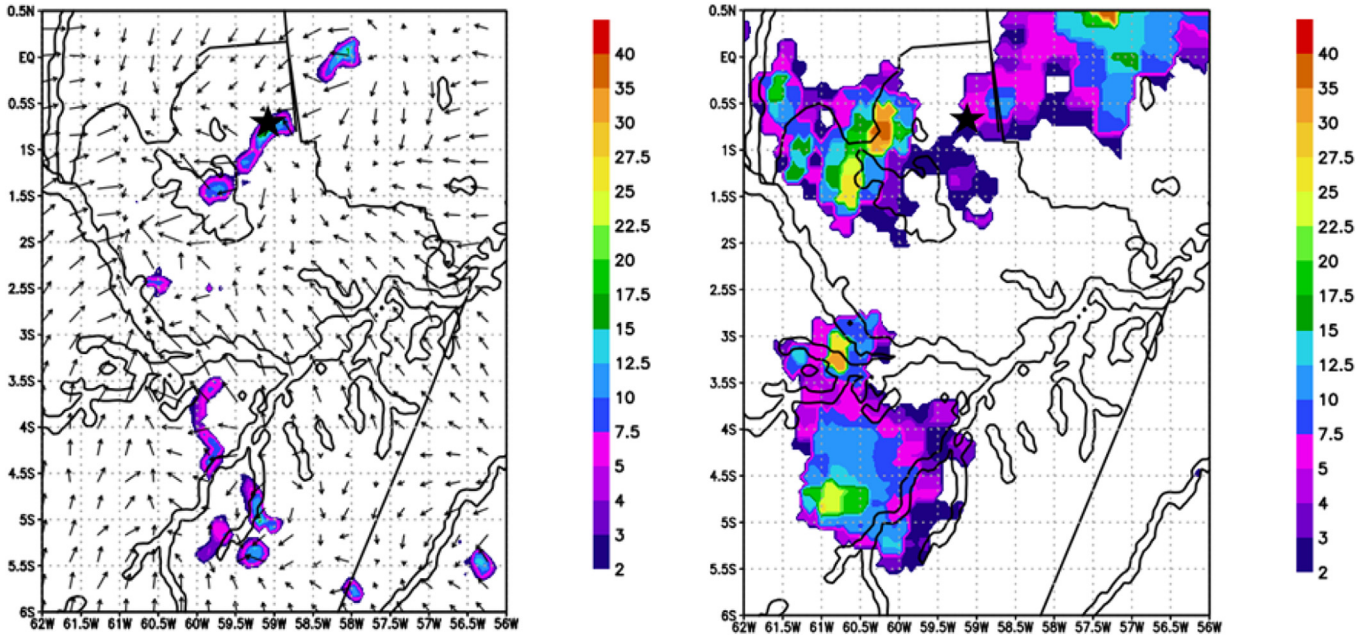

Fig. 3. (a) Precipitation rate (mm h^{-1}, shading) and Horizontal wind (m s^{-1}, vector) at 43.9 m obtained by the JULES-CCATT-BRAMS model on April 14, 2014 at 08 UTC. (b) Precipitation rate obtained by CMORPH (mm h^{-1}). Black star indicates the position where the precipitation rate was more intense (0.70° *S* 59.10° *W*).

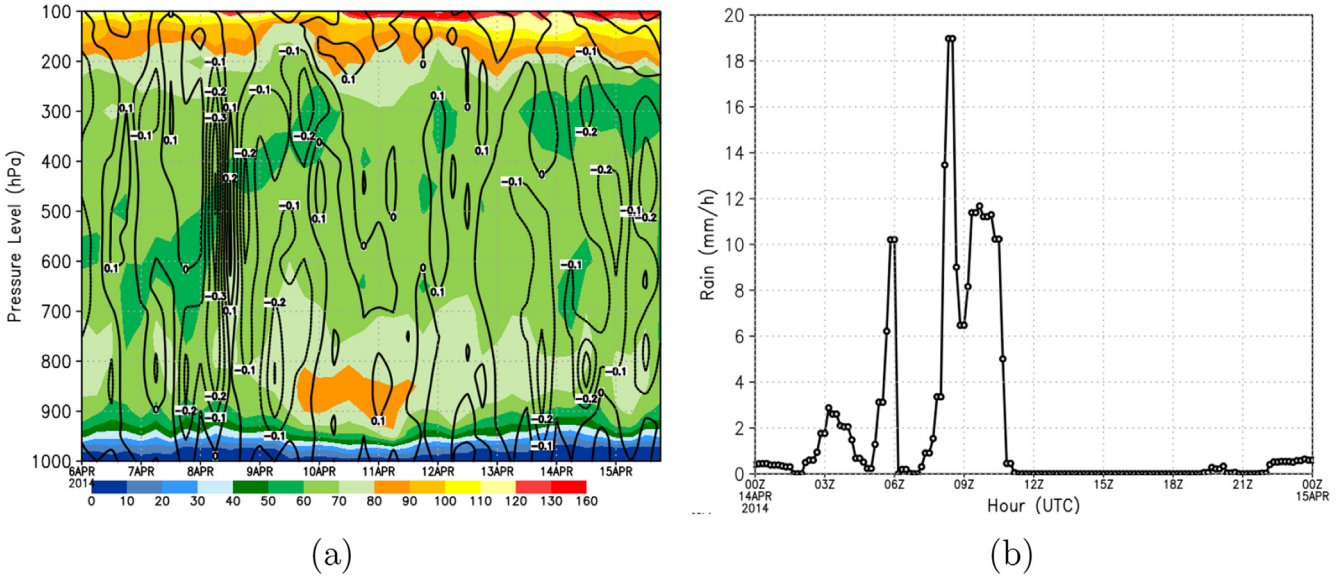

Fig. 4. (a)Vertical cross section of the ozone concentration (ppbv, shading) and vertical velocity (black line) obtained from the reanalysis of the ECMWF Era-Interim. (b) Distribution of precipitation rate (mm h^{-1}) during April 14, 2014, where the precipitation rate was more intense (0.70° *S*59.10° *W*).

simulation.

3.1. Description of the case study

Satellite images were used in order to verify the kinds of convective systems that passed through Central Amazon region between April 10–14, 2014. On April 14 two SL formed and passed over Manacapuru (Fig. 2). The first SL formed in the early hours of the morning before dawn on April 14th (Fig. 2c), while the second SL formed during the afternoon (not shown). The SL that formed in the early hours of the morning before dawn is the object of the present analysis since during this time of day the effects of solar radiation are absent, and this facilitates the evaluation of just the passage of the convective system and its effects on O_3.

During the day before the formation of the SL (April 13), at 21 UTC (local time = UTC - 4 h) there was a large concentration of isolated convective cells above the State of Pará, and the formation of convection aligned with a FS above the southeast of South America, reaching the south of the State of Amazonas (Fig. 2a). At 00 UTC on April 14 the convection weakened above Pará and the south of Amazonas, and shortly thereafter at 0230 UTC (Fig. 2b), the SL began to organize itself and take shape, and its direction was from the northwest of the State of Pará to the southeast of the State of Amazonas. At 0430 UTC the SL was moving to the west, and at 0730 UTC it arrived over the Central Amazon region (Fig. 2c). At 12 UTC the SL initiated its dissipation, having completely lost its linear formation at 15 UTC on April 14. Finally, at 18 UTC (not shown) the linear formation of a new SL was observed, and it intensified at 19 UTC and dissipated at 2230 UTC.

The analysis of the synoptic chart for the surface on April 14 at 00 UTC (http://tempo.cptec.inpe.br/boletimtecnico/pt) shows a large

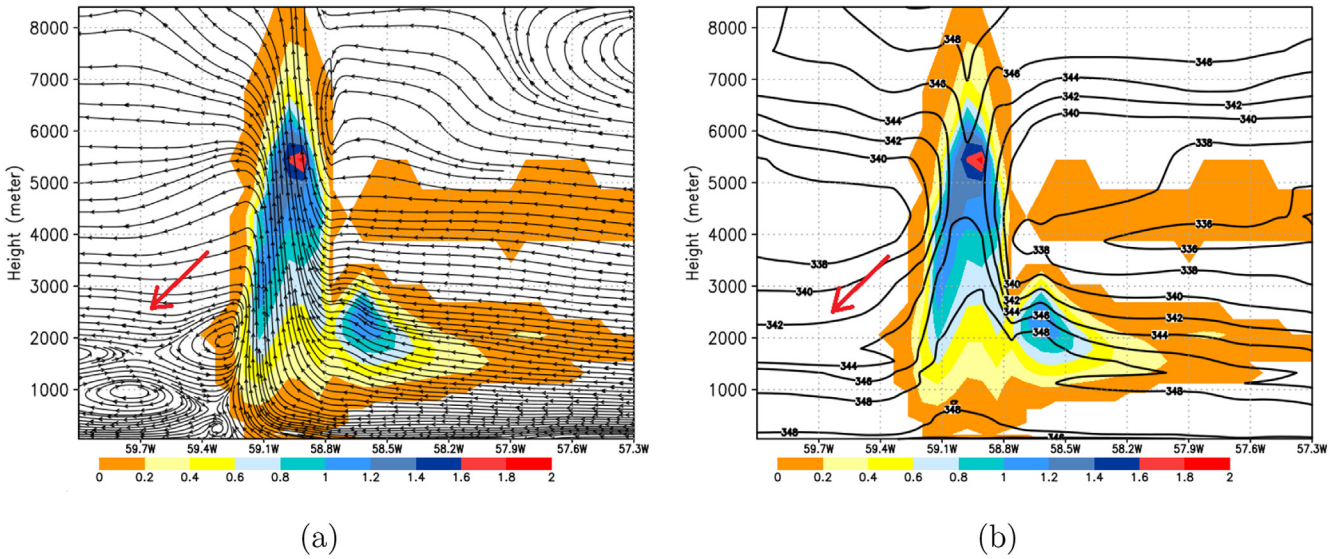

Fig. 5. Vertical cross section at 0.70° S, at 08 UTC on April 14, 2014 for (a) cloud mixing ratio (gk g^{-1}, shading) and streamlines of u, w and (b) cloud mixing ratio (gk g^{-1}, shading) and equivalent potential temperature (K, black line).

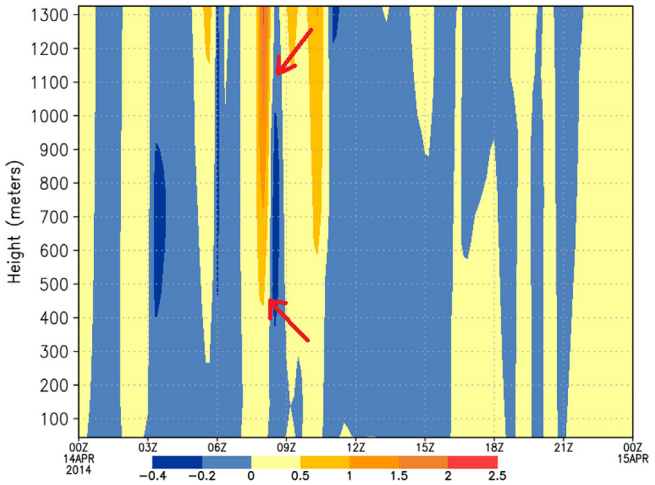

Fig. 6. Vertical cross section of the vertical wind (m s^{-1}, shaded) during April 14, 2014, where the precipitation rate was more intense (0.70° S − 59.10° W). The red arrows indicate updrafts and downdrafts observed around 08 UTC. (For interpretation of the references to color in this figure legend, the reader is referred to the Web version of this article.)

scale environment before the formation of the SL during the early morning hours before 14th April's dawn. There was an intense extra-tropical cyclone over the southern Atlantic and a cold front that extended from the southeastern coastal area of Brazil to Bolivia (not show). The presence of this FS favored the formation of a convergence zone of humidity from the State of São Paulo to the State of Acre (not show).

Several studies have reported that there is an increase in convective activity in the Amazon due to the penetration of frontal systems into the region, and this could be associated to the structural characteristics of convective systems (Siqueira and Machado, 2004; Siqueira et al., 2005; Negrón-Juárez et al., 2010, 2017). Siqueira et al. (2005) analyzed three types of interactions above South America between tropical convection and frontal systems in the mature phase. According to these authors, there is a need to conduct the analyses of these phenomena in two different latitudinal zones, in the tropics and the subtropics, due to the necessity to investigate such interactions in two different synoptic configurations: fronts that initially penetrate above South America (interacting with convection principally in the subtropics), and fronts interacting with tropical convection, due to the fact that the latter move directly to the lower latitudes of the tropics, or due to the establishment of incursions of cold air above the tropics. The study by Siqueira et al. (2005) was a continuation of a previous study by Siqueira and Machado (2004) that concluded that there are three different types of interactions between humid air in the tropics and incursions of cold air masses in the middle latitudes.

Based on the classification proposed by Siqueira and Machado (2004) and on the analysis of the satellite images from April 11 to 16, it can be affirmed that the interactions between FS and the convection that gave rise to the SL on April 14 can be classified as type 1. In a type 1 interaction penetration of frontal systems from the subtropics or the middle latitudes is frequent, and these serve to organize convective activity in the tropics and move to the north to lower tropical latitudes with the convection.

3.2. Simulation of the squall line

The results for the simulated rainfall rate crosschecked with the precipitation rate estimated with CMORPH showed that the model was able to satisfactorily capture the formation of the SL that formed in the early morning hours before dawn on April 14th (not shown). Fig. 3a shows the simulated results for the convective precipitation rate (CPR) and the horizontal wind at a height of 43.9 m (closest surface level available in the simulation results) at 08 UTC, when the SL was in the central Amazon region at its mature phase.

It is observed that the precipitation rate simulated (Fig. 3a) was underestimated when compared to the precipitation rate extracted from the CMORPH (Fig. 3b). However, the model estimated rate was similar to that found in CMORPH, which is also comparable to that previously observed in GOES 13 satellite images (2c). Thus, this time will be used for analysis that will be presented from this point forward. Besides that, this point (black star in Fig. 3a) will be the reference point where the convective activity of the SL was more intense (0.70° S 59.10° W) and will be denominated the most active point of convection.

3.3. Aspects of the most active point of convection

Initially, in this section particular attention will be given to the levels of tropospheric O_3 in the region of the most active point of convection. Fig. 4a show the vertical profile of O_3 and the vertical component of the wind. The data were extracted from the ECMWF Era-

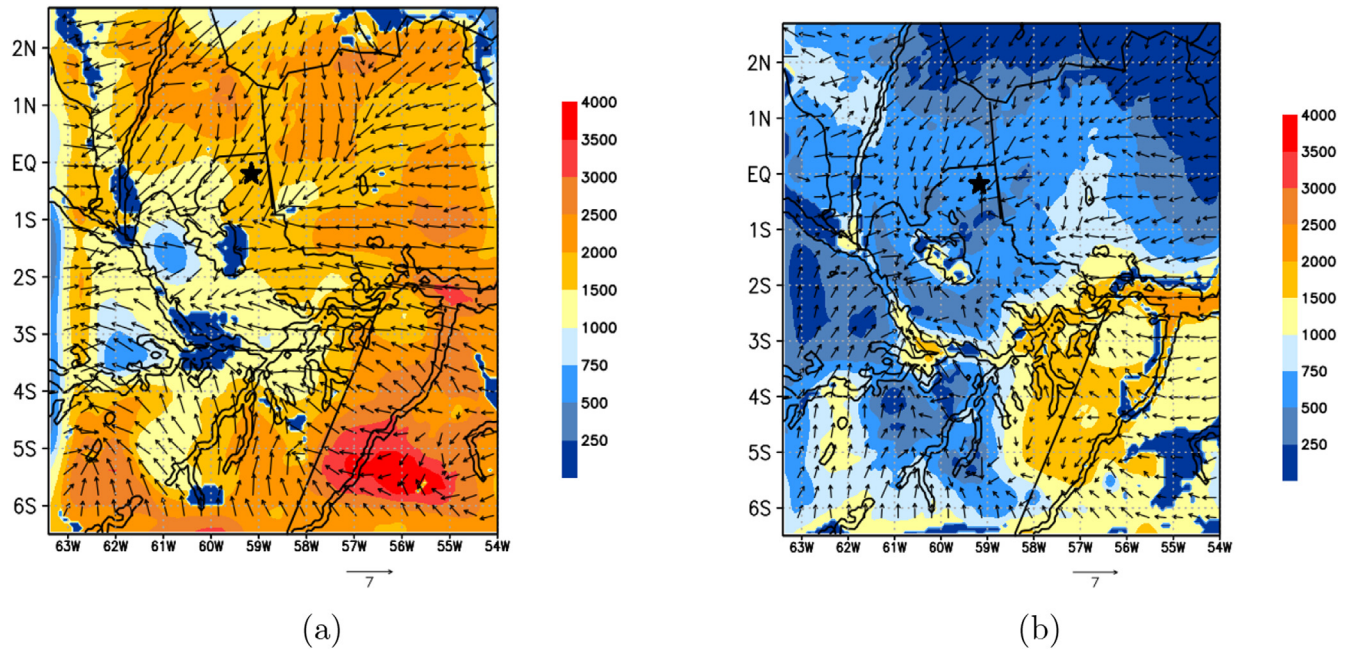

Fig. 7. Horizontal distribution of CAPE (Jkg^{-1}, shaded) and horizontal wind (m s^{-1}, vector) at 43.9 m for April 14, 2014 at (a) 00 UTC and (b) 08 UTC.

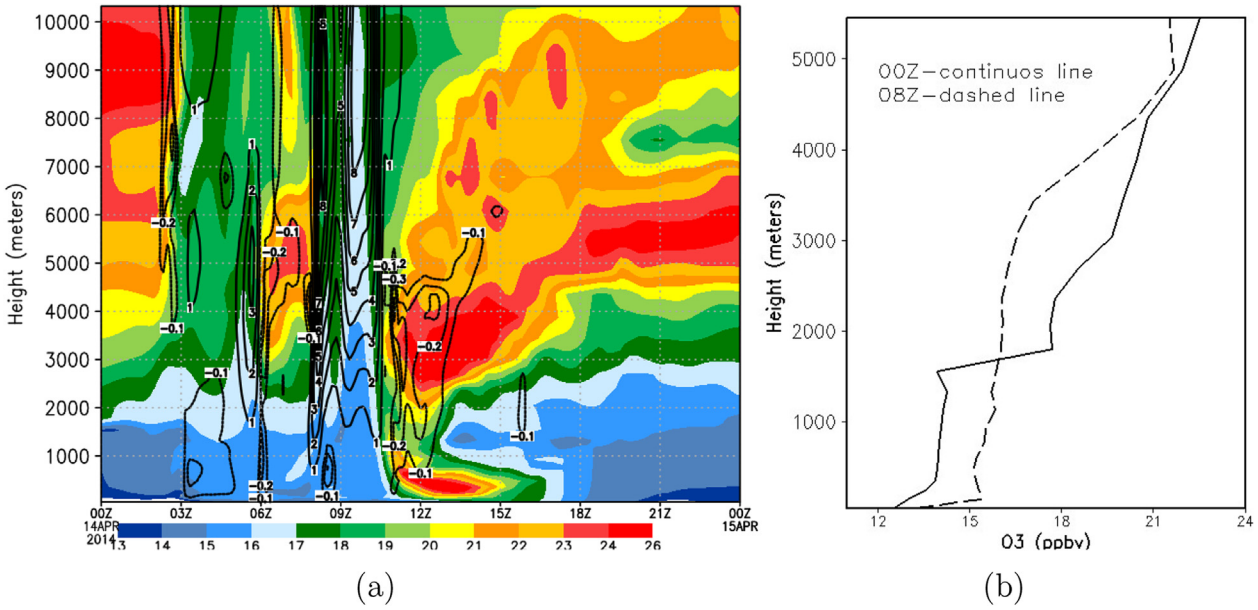

Fig. 8. (a) Cross section of ozone concentration O_3 (ppbv) and vertical velocity (m s^{-1}) (black line) at the most active point of the storm (0.70° *S* - 59.10° *W*), during April 14 and (b) vertical profiles of O_3, at 00 UTC (continuous line) and 08 UTC (dashed line).

Interim dataset for the days of April 6 to 15, 2014. The O_3-levels varies from 10 to 50 ppbv in the lower troposphere (between 1000 and 900 hPa) during the entire period. However, the higher O_3-levels reach 90 ppbv in the middle troposphere between April 10–14, forming a plume of O_3 that extends from the level of 950 hPa up to 650 hPa. During this period the O_3 concentration was larger than the ones obtained for the other analyzed days. On April 14 the O_3-levels reached values near 80 ppbv in the middle troposphere, and there were ascending and descending vertical currents in the plume (black line) associated with convective activity of the SL.

Fig. 4b shows the convective precipitation rate simulated by the JULES-CCATT-BRAMS model at the most active point of convection, during the entire day on the 14th of April. The rainfall that occurred at this site began at 02 UTC and reached a maximum of 19 mm h^{-1} at 0820 UTC, and ended around 11 UTC. The model reproduced a storm associated with the SL that will be considered as a reference in the analyses conducted in this study.

3.4. Vertical structure of the atmosphere and vertical ozone transport during the passage of a squall line

The analyses in this section were conducted using as a base the modifications caused by the passage of the SL with respect to the vertical structure of the troposphere as well as the vertical transport of O_3, from middle troposphere (plume of O_3) to the surface (Fig. 4a).

Fig. 5a shows a vertical cross section of cloud mixing ratio and streamlines of the zonal and vertical wind components at latitude 0.70° *S* at 08 UTC on April 14. Fig. 5b, which is similar to Fig. 5a, the

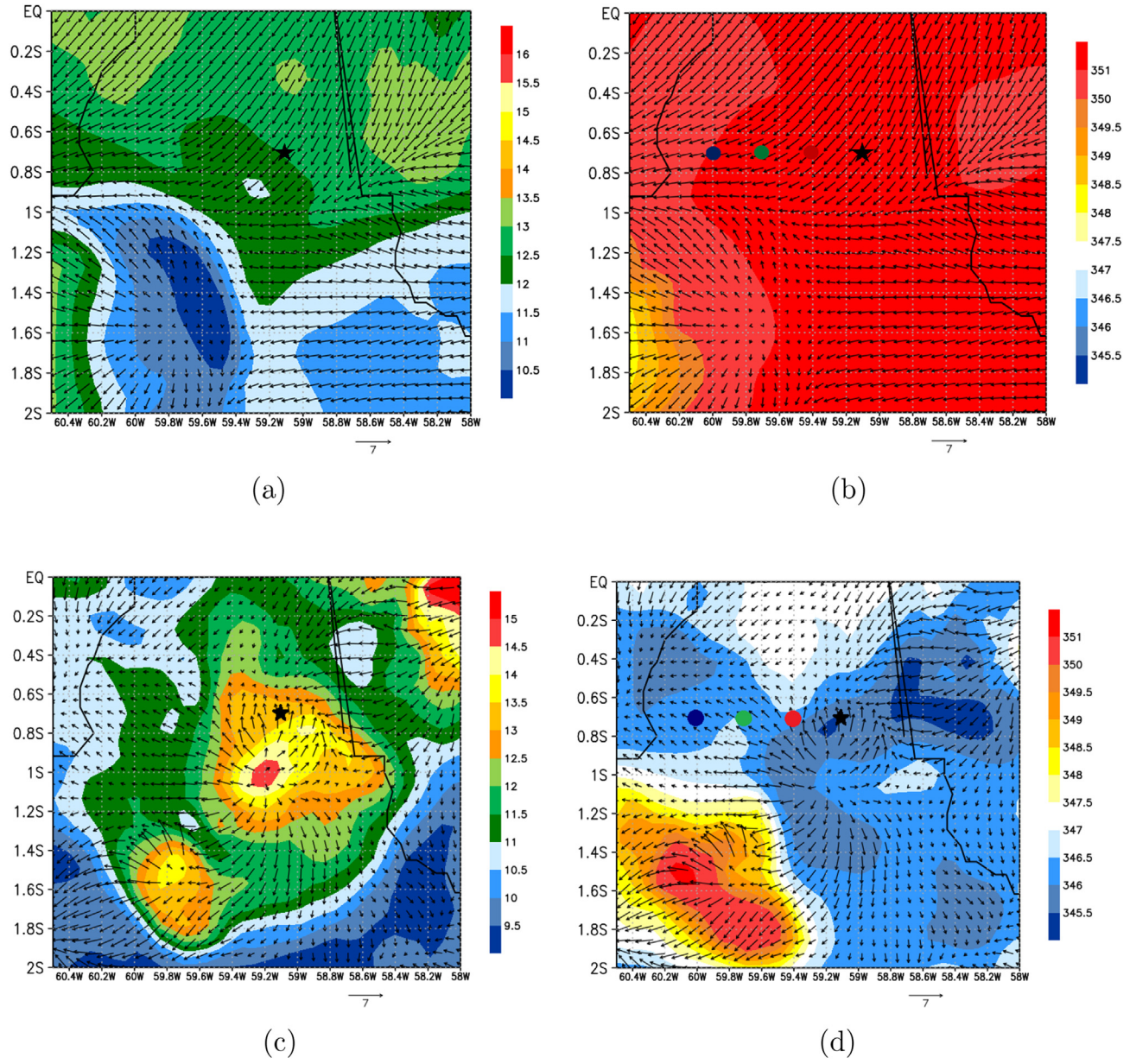

Fig. 9. Horizontal distribution of ozone (a,c) (ppbv, shading) with horizontal wind (m s^{-1}, vector) at 00 and 08 UTC, respectively. Equivalent potential temperature (b,d)(K, shading) with horizontal wind (m s^{-1}, vector) at 00 and 08 UTC, respectively, at 43.9 m on April 14, 2014. The black star represents the position where the precipitation rate was more intense (0.70° *S* 59.10° *W*) and the colored circles correspond to: 0.70° *S* 59.40° *W* (red), 0.70° *S* 59.70° *W* (green) and 0.70° *S* 60.00° *W* (blue). (For interpretation of the references to color in this figure legend, the reader is referred to the Web version of this article.)

black lines represent θ_e values.

Fig. 5a shows that the SL system is composed of mature cells with a high value for the mixing ratio, and that the zonal wind is predominantly easterly with convergence at low levels. Additionally, updrafts generated by the SL rise up to the anvil-shaped top of the cloud, while the downdrafts are observed at lower levels in front of the system from the surface to about 2,500 m (red arrow in Fig. 5a). When the downdraft reaches the ground the cold air spreads out in all directions forming what is conventionally called a density current (or gravity current), which replaces hot, humid air at the layer at the base of the cloud (Costantino and Heinrich, 2014).

The distribution of θ_e values and the cloud mixing ratio suggest that the passage of the SL caused cooling and drying in the lower and middle troposphere. This result is in agreement with the conceptual model of an SL proposed by Garstang et al. (1994). Additionally, in the region of the downdrafts there was a gradual decrease from 348 K to 342 K in the θ_e values (red arrow in Fig. 5b). This cooling is probably a consequence of the action of the downdrafts and the subsequent presence of the density current, the effects of which can be seen by examining the fields of meteorological variables near the surface (not show here) (Zipser, 1977; Betts et al., 2002; Costantino and Heinrich, 2014).

The vertical wind velocity at the most active point of the storm during April 14 is presented in Fig. 6. Ascending (positive) and descending (negative) movements of air are seen during the entire day, but mainly during the early morning hours before dawn on April 14 when these were much more intense. There were strong ascending and descending movements of air especially near 08 UTC, the time in which the SL was above the site. These increases in the absolute value of the vertical velocity are typical characteristics of updrafts and downdrafts generated by the SL when it passed through the region.

Fig. 7 shows the horizontal distribution of CAPE (potential energy available for convection) at 00 UTC (Fig. 7a, before SL formation) and

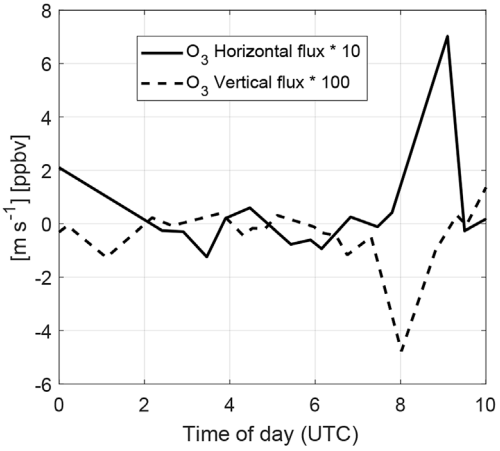

Fig. 10. Horizontal transport of ozone (continuous line) calculated at 0.50° *S* - 59.10° *W* and vertical transport of ozone (downdraft, dashed line) calculated at the most active point of convection (0.70° *S* - 59.10° *W*). Both transports were calculated through the simulations of JULES-CCATT-BRAMS from 00 to 10 UTC on April, 14.

at 08 UTC (Fig. 7b, when the SL is already formed). At the most active point of the storm (black star) the value of CAPE is approximately 1,700 Jkg^{-1} at 00 UTC, indicating a tendency for development of deep convection, since a value of CAPE of 1,000 Jkg^{-1} is commonly considered to be the threshold for the irruption of such an event. Values of CAPE between 1,000 and 3,000 Jkg^{-1} are associated with a type of convection classified as moderate to intense (Machado et al., 2004; Mota and Nobre, 2006). At 08 UTC it is evident that the CAPE values are on the order of 500 Jkg^{-1} in the center of the storm, and this would be expected since it is known that the CAPE value decreases considerably once the convection is formed, and this can occur in an abrupt manner (Machado et al., 2004).

Chase et al. (2016) showed that there is a significant correlation between the values of CAPE before a storm and the O_3-enhancement events near the surface. Furthermore, Dias-Júnior et al. (2017) showed that a reduction in the CAPE values that occur during strong convective activity are more highly correlated with O_3-enhancement events near the surface than with a reduction in the values of θ_e.

Fig. 8a present transversal sections of O_3 concentrations, during April 14, 2014. Fig. 8b show the simultaneous vertical profiles of concentrations of O_3, at 00 UTC and 08 UTC, the hours before and after the development of the SL. In Fig. 8a a greater concentration of O_3 is evident in the middle troposphere (around 26 ppbv), approximately at the same level as the O_3 plume observed in Fig. 4a. Additionally, the movement of the downdrafts (black dashed line) brought a large quantity of O_3 in the direction of the surface. In addition, in Fig. 8b it is possible to note that at 08 UTC (during the downdraft) compared to 00 UTC, the O_3-level decrease in the region between 2000 and 5000 m and increased at low levels.

Also in Fig. 8a, in the interval just before 12 UTC to 15 UTC, there was a considerable increase in the transport of O_3 from the middle troposphere into the surface, and this vertical flux of O_3 occurred in the presence of strong downdrafts. The results of the simulation for April 14 show that at 12 UTC the dissipation of the SL had already occurred (not shown). However, an isolated cloud was observed near 12 UTC which caused strong downdrafts at this point.

3.5. The horizontal ozone transport during the passage of a squall line

In this section the O_3 route, immediately after reaching the surface via downdraft will receive particular attention. The hypothesis suggested by Dias-Júnior et al. (2017) will be verified, that is, if O_3 is transported on the surface by LLJ, which originate from the presence of density currents.

In Fig. 9a, c the horizontal distribution of O_3-levels is shown at 00 and 08 UTC, respectively. Fig. 9b,d shows the θ_e values at 00 and 08 UTC, respectively. The arrows in Fig. 9a–d correspond to the horizontal wind near the surface and the black star is the most active point of convection. At 00 UTC, before the presence of the SL, it is possible to notice that O_3-levels were approximately 12 ppbv (Fig. 9a) and the θ_e value were close to 350 K (Fig. 9b) at the most active point of convection. In addition, the easterly and northeasterly winds predominate. However, at 08 UTC the values of O_3 near the surface are high, with a maximum near the region located at 1.10° *S* 59.20° *W* (Fig. 9c). Furthermore, in this region there is also a divergence of the horizontal wind near the surface. There are also high O_3-levels near the surface in other regions such as near the Equator and at the latitude 1.60° *S*. Such regions appear to be associated with the presence of convective cells that are elements that are integrated into the simulated SL.

In the region of the storm center (black star, Fig. 9d), the values of θ_e

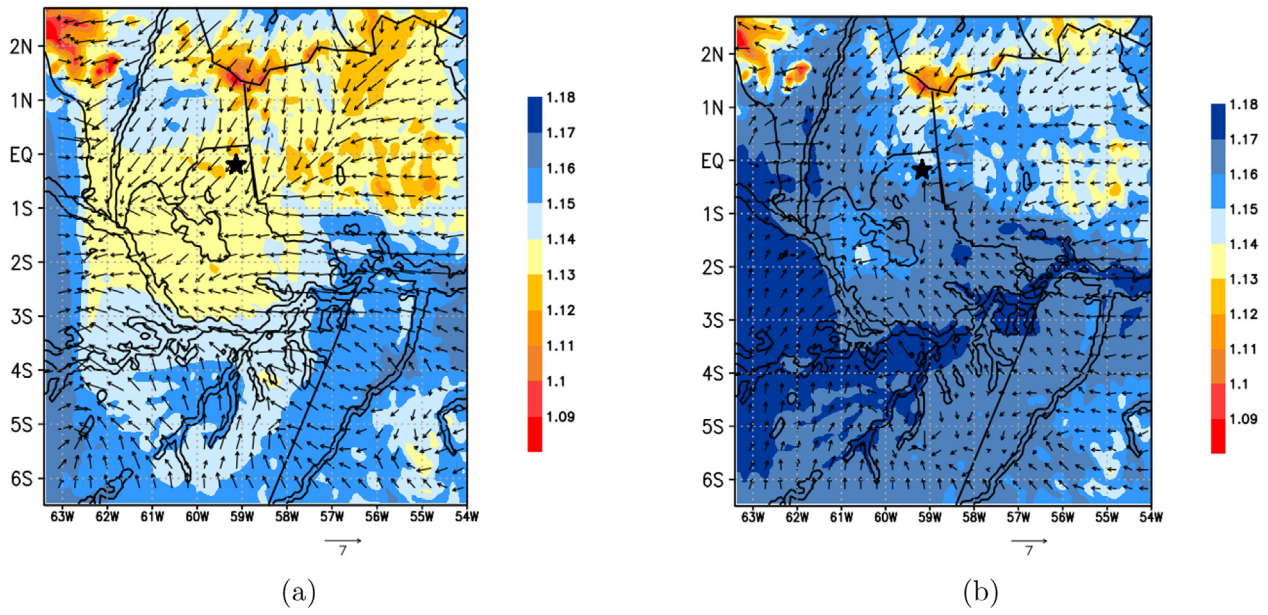

Fig. 11. Horizontal distribution of air density (kg m^{-3}) and horizontal wind (m s^{-1}, vector) at 43.9 m for April 14, 2014 at (a) 00 UTC and (b) 08 UTC.

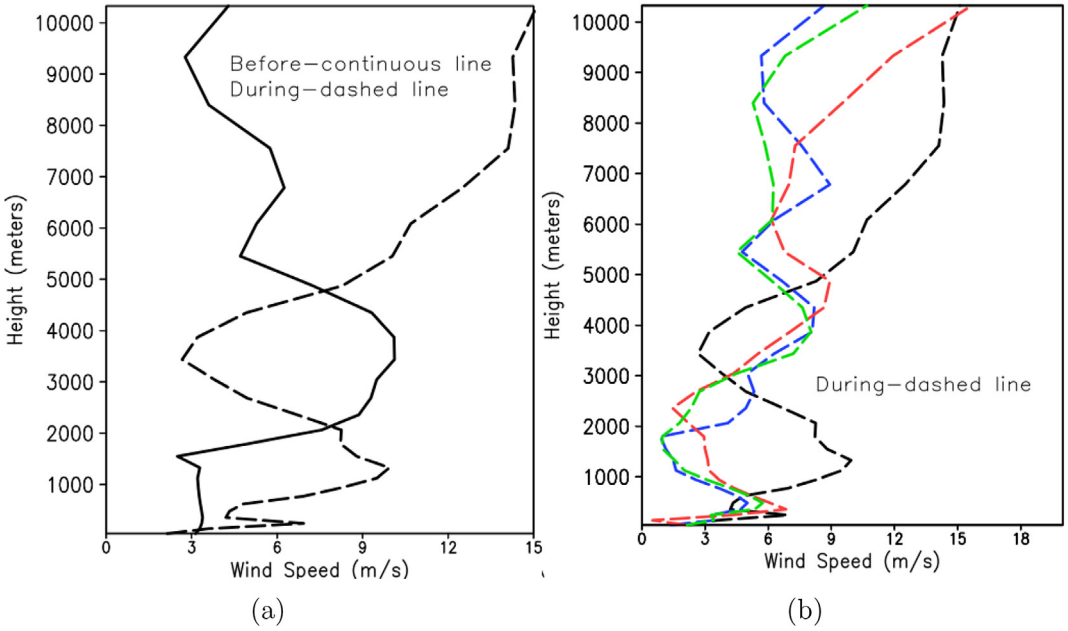

Fig. 12. Vertical cross section of horizontal wind (m s^{-1}) during April 14, 2014 (a) where the precipitation rate was more intense (0.70° S - 59.10° W), at 00 UTC (Before - continuous line) and 08 UTC (During - dashed line), and (b) at 08 UTC at latitude 0.70° S for differents longitudes: 59.10° W (black line), 59.40° W (red line), 59.70° W (green line) and 60.00° W (blue line), these points were indicated in Fig. 9b. (For interpretation of the references to color in this figure legend, the reader is referred to the Web version of this article.)

are about 2 K less in comparison with the values calculated in neighboring regions. This indicates that at the time around 08 UTC a parcel of cold, dry air that originated in a downdraft reached the surface. Additionally, in the same region there is a clear flow divergence near the surface. Therefore, it is suggested that these simulations succeeded in reproducing quite well the following dynamic features: downdrafts associated with the SL reached the surface and were responsible for the O_3-enhancement events at the surface (Fig. 9c), and also for the θ_e reduction due to the transport of material that originated in the upper layers of the troposphere, as also observed by Betts et al. (2002) and Gerken et al. (2016) in their studies on the action of downdrafts above the Amazon forest.

Dias-Júnior et al. (2017), in their study on the action of convective storms on the dynamics of the atmosphere of Amazonia, suggested that air that is colder and richer in O_3, originated in the upper layers of the atmosphere from where it was brought by downdrafts, formed a density current when it reached near to the surface, and propagated itself in the form of a LLJ. These authors referred to such jets as “non-classic”, but upon concluding their article they did not possess sufficient data to prove this hypothesis.

In contrast, this same hypothesis of Dias-Júnior et al. (2017) is supported in the present study as a result of the simulations conducted using the JULES-CCATT-BRAMS model. Fig. 10 shows the downdraft flux (O_3 vertical flux) and its lateral transport (O_3 horizontal flux). For the calculation of O_3 vertical flux ($\overline{w'O'_3}$) simulation results at the nearest level to the surface (43.9 m) was used. We chose the most active point of convection (0.70° S - 59.10° W) to calculate the values of $\overline{w'O'_3}$.

A method similar to the eddy covariance method was used to obtain $\overline{w'O'_3}$ that is, w' was considered to be the fluctuation of the vertical wind speed around its mean value. The average vertical wind speed ($\bar{w}$) was found by arithmetic mean of all values of w from 00 to 10 UTC on April 14, 2014. From 10 UTC the O_3 values tend to increase due to sunrise and therefore they were not used. O'_3 is the fluctuation of ozone around its mean value ($\overline{O_3}$). The values of O'_3 were obtained in a manner similar to the values of w'.

For the calculation of the O_3 horizontal flux ($\overline{u'O'_3}$), simulation results were used at the closest surface level (43.9 m) at the point (0.50° S - 59.10° W) next to the most active point of convection. The methodology used for the calculation of $\overline{u'O'_3}$ was similar to that used for the calculation of $\overline{w'O'_3}$. The distance between $\overline{u'O'_3}$ and $\overline{w'O'_3}$ calculation was approximately 23 km.

Around 08 and 09 UTC the $\overline{w'O'_3}$ and $\overline{u'O'_3}$ values were considerably larger, respectively, when compared to the values obtained at other times (Fig. 10). This 1 h delay between the maximum values of $\overline{w'O'_3}$ and $\overline{u'O'_3}$ was already expected since these fluxes were calculated at grid point of approximately 23 km. Therefore, it is possible to conclude that part of the increase of O_3 observed at the point 0.50° S - 59.10° W occurred due to a horizontal transport of O_3 coming from adjacent regions, where frequent downdrafts occurred.

There is an increase of air density (ρ) value during 00 and 08 UTC, as shown in Fig. 11a and b, respectively, at the same time of rainfall caused by the SL. The value of ρ increase from 1.14 kg m^{-3} (00 UTC) to 1.17 kg m^{-3} (08 UTC) at the most active point of convection (black star). As previously stated, sudden increases in ρ values at the surface, accompanied by a reduction in θ_e values and an increase in the horizontal wind velocity, besides changes in wind direction, are typical signs of the incidence of density currents generated by cold air originating in downdrafts from tropical storms (Costantino and Heinrich, 2014; Dias-Júnior et al., 2017).

Fig. 12a shows the horizontal wind profiles (U) at the most active point of convection before and after the formation of the simulated SL at 00 UTC and 08 UTC, respectively. Fig. 12b show the horizontal wind profile at 08 UTC for longitudes near the most active point of convection (59.40° W, 59.70° W, 60.00° W).

The values of horizontal wind did not show abrupt changes at 00 UTC. However, at 08 UTC there was a significant increase in U values at low levels in the atmosphere (Fig. 12b), and also the formation of a LLJ that reached a velocity of 6.5 m s^{-1} and a height of approximately 250 m, and covered a distance of approximately 67 km (from 59.10° W to 59.70° W), with an approximate velocity of 5.5 m s^{-1}. As demonstrated by the results presented up to this point in this paper, the existence of these jets is a consequence of the development of density currents generated near the surface in the region where the downdrafts occur. This conclusion is supported by the results of Dias-Júnior et al. (2017), who suggested that the LLJs are products of the development of density currents in the air above the tropical regions. Furthermore, they showed

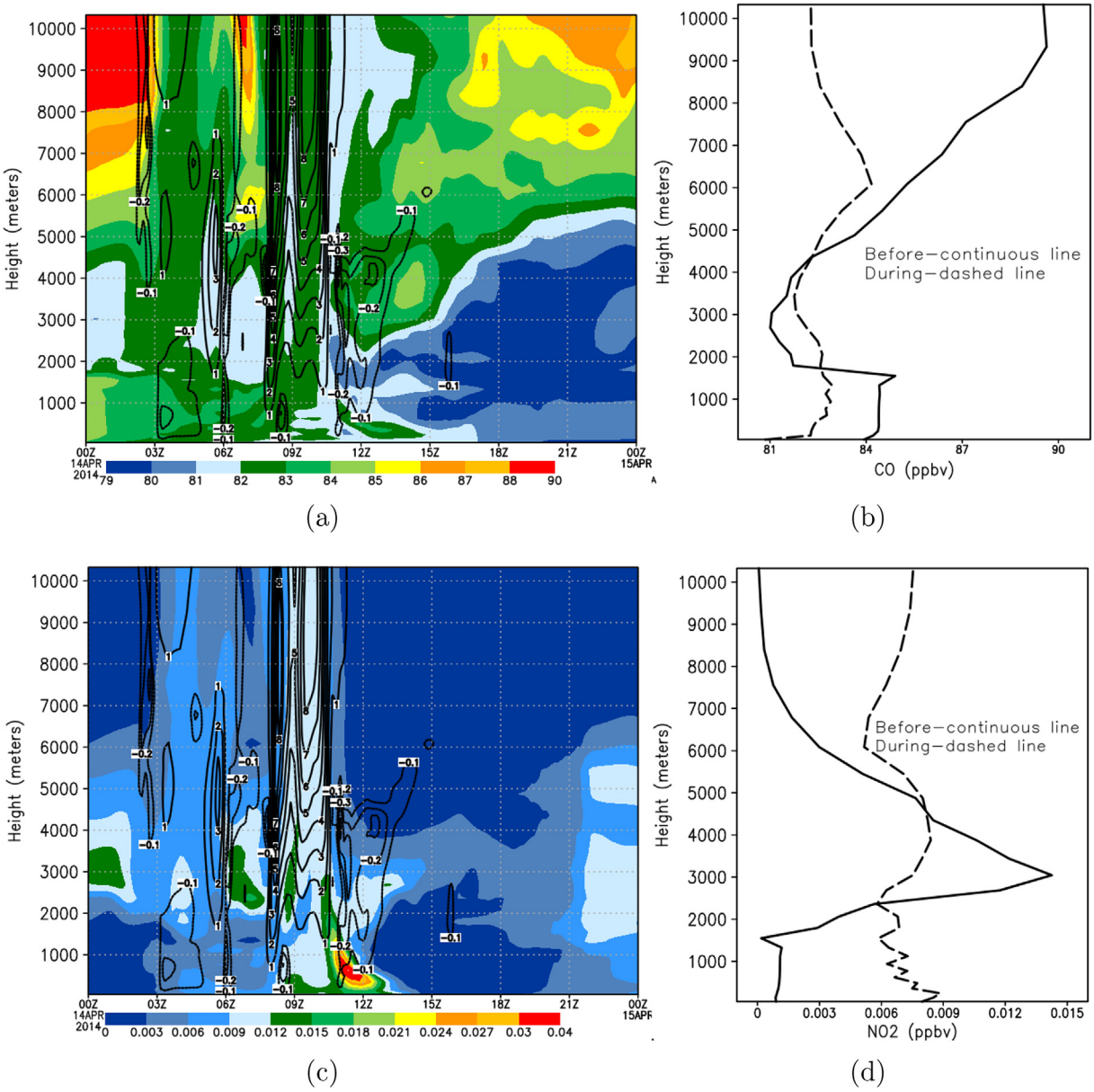

Fig. 13. Cross section of gas concentration (a) CO (ppbv) and (c) NO_2 (ppbv) and vertical velocity (m s^{-1}) (black line) during April 14, 2014 at the most active point of the storm (0.70° *S* - 59.10° *W*), and vertical profiles of (b) CO and (d) NO_2 at 00 UTC (continuous line) and 08 UTC (dashed line).

that in situations of the O_3-enhancement events above the surface, there was a high frequency of occurrence of these jets.

3.6. Other gases during the passage of an squall line

Fig. 13a, c presents transversal sections of carbon monoxide (CO) and nitrous oxide (NO_2) concentrations, respectively, during April 14, at the most active point of the storm. Fig. 13b,d shows the simultaneous vertical profiles of concentrations of CO and NO_2 at 00 UTC and 08 UTC, the hours before and after the development of the SL.

In Fig. 13a there is a reduction in the CO values (−10 ppbv) as the downdrafts approach the surface, indicating that these descending movements are cleaning the air, and for this reason there is a reduction of CO at low levels (−4 ppbv) (Freitas et al., 2005). This is corroborated by Fig. 13b, since at 00 UTC the CO values in the lower troposphere are greater than that observed at 08 UTC.

Fig. 13c shows the vertical profile of NO_2 on April 14. The interesting aspect of this profile is that the average NO_2 level remains low during almost the entire day (from 0.003 to 0.009 ppbv). However, small increases in concentration are observed in the lower and middle troposphere only during the hours when the downdrafts occurred, reaching a maximum of 0.040 ppbv near the surface.

The large O_3 level in the middle troposphere and the increase in the concentration of this gas near the surface could have caused an increase in the concentration of NO_2 since O_3 reacts with nitric oxide (NO) forming NO_2 and molecular oxygen (O_2) (Gerken et al., 2016). In Fig. 13c the increase in the concentration of NO_2 is seen at 08 UTC.

It is worth mentioning that these numeric simulations with the JULES-CCATT-BRAMS model allowed for a better understanding of the tridimensional structure of the dynamics of chemical and thermodynamic aspects of the atmosphere during the passage of the SL. This research has shown that the downdrafts caused by the SL brought cold air that was rich in O_3 from the middle troposphere to the terrestrial surface where density currents were formed and spread out in the form of LLJs and subsequently dispersed in a radius of approximately 70 km from the core of the downdraft. Additionally, the air downdrafts had lower concentrations of CO, and the greater levels of O_3 at the surface promoted other chemical reactions such as the formation of NO_2.

4. Conclusion

In this study, specific processes related to the organization of deep convection above the Amazon forest in the tropical region of South America were studied. The study used numerical simulations with the JULES-CCATT-BRAMS model which allowed for a better understanding of the tridimensional structure of the dynamics of chemical and thermodynamic aspects of the atmosphere during the rainy season in the region. Special attention was given to the analysis of squall lines (SL) that form in the interior of the continent. In contrast to classic SL that form on the Atlantic coast due to the marine breeze, and that after forming penetrate into the interior of the continent, the SL studied here form in the interior of Amazonia and are accompanied by strong episodes of convection which are able to maintain a degree of synergy with the development of deep convection in the South Atlantic Convergence Zone. These SL have the capacity to alter chemical aspects and the thermodynamic structure of the middle and lower troposphere through which they pass.

It was shown that during the passage of a SL the downdrafts, originated in this convective system, were responsible for sudden increases in the concentration of ozone, horizontal wind velocity, air density among other physical and chemical parameters. Moreover, rapid decreases in equivalent potential temperature were observed in the presence of these downdrafts.

Through the use of reanalysis data from the ECMWF Era-Interim dataset it was possible to describe a “plume” rich in ozone in the middle troposphere. It was concluded that substantial increases in the concentration of ozone near the surface occur when downdrafts from the SL pass through the “plume” and bring ozone from the middle troposphere. Also, this analysis demonstrated that the downdrafts induced the formation of density currents that spread out in the form of low-level jets and are capable of transporting gaseous chemical compounds over large distances.

Acknowledgements

The authors thank the European Center for Medium-Range Weather Forecasts (ECMWF) for the reanalysis data, and the Center for Weather Prediction and Climate Studies (Centro de Previsão de Tempo e Estudos Climáticos (CPTEC/INPE) for providing the JULES-CCATT-BRAMS model. Furthermore, the authors thank the Amazon Modeling Laboratory (Laboratório de Modelagem da Amazônia, LAMAZ) for the technical help given, the Brazilian Research Council (CNPq, Conselho Nacional de Desenvolvimento Científico e Tecnológico) for the Masters scholarship and also PROPESP/UFPA (programa de apoio à publicação qualificada - PAPQ < 2018).

Appendix A. Supplementary data

Supplementary data to this article can be found online at https://doi.org/10.1016/j.atmosenv.2019.02.018.

References

Alcântara, C.R., Dias, M.A.S., Souza, E.P., Cohen, J.C., 2011. Verification of the role of the low level jets in amazon squall lines. Atmos. Res. 100 (1), 36–44. http://www.sciencedirect.com/science/article/pii/S0169809510003704.

Alcântara, C.R., Souza, Ê. P. d., Dias, M. A. F. d. S., Biazeto, B., 2014. Influência dos jatos em médios e baixos níveis nos processos de nuvem: Estudo numérico de uma linha de instabilidade amazônica. Revista Brasileira de Meteorologia 29 (1), 29–46.

Best, M.J., Pryor, M., Clark, D.B., Rooney, G.G., Essery, R.L.H., Ménard, C.B., Edwards, J.M., Hendry, M.A., Porson, A., Gedney, N., Mercado, L.M., Sitch, S., Blyth, E., Boucher, O., Cox, P.M., Grimmond, C.S.B., Harding, R.J., 2011. The joint uk land environment simulator (jules), model description–part 1: Energy and water fluxes. Geosci. Model Dev. (GMD) 4 (3), 677–699. https://www.geosci-model-dev.net/4/677/2011/.

Betts, A.K., Gatti, L.V., Cordova, A.M., Dias, M.A.S., Fuentes, J.D., 2002. Transport of ozone to the surface by convective downdrafts at night. J. Geophys. Res.: Atmosphere 107 (D20) LBA–13.

Chase, R.J., Fuentes, J.D., Gerken, T., Wei, D., Schumacher, C., Santos, R.M.N., Martin, S.T., Springston, S., 2016. Convection and redistribution of tropospheric ozone in central amazonia. In: 15th Annual Student Conference, American Meteorological Society, 10-14 January, New Orleans, LA.

Clark, D.B., Mercado, L.M., Sitch, S., Jones, C.D., Gedney, N., Best, M.J., Pryor, M., Rooney, G.G., Essery, R.L.H., Blyth, E., Boucher, O., Harding, R.J., Huntingford, C., Cox, P.M., 2011. The joint uk land environment simulator (jules), model description–part 2: Carbon fluxes and vegetation dynamics. Geosci. Model Dev. (GMD) 4 (3), 701–722. https://www.geosci-model-dev.net/4/701/2011/.

Cohen, J.C.P., Dias, M.A.F.S., Nobre, C.A., 1995. Environmental conditions associated with amazonian squall lines: A case study. Mon. Weather Rev. 123 (11), 3163–3174. https://doi.org/10.1175/1520-0493(1995)123<3163:ECAWAS>2.0.CO;2.

Costantino, L., Heinrich, P., 2014. Tropical deep convection and density current signature in surface pressure: comparison between wrf model simulations and infrasound measurements. Atmos. Chem. Phys. 14 (6).

Crutzen, P.J., 1987. Role of the tropics in atmospheric chemistry. John Wiley for the United Nations University.

Davis, D., 1973. Influence of thunderstorms on environmental ozone. In: Proceedings of the Annual Tall Timbers Fire Ecology Conference, vol. 13. pp. 505–516.

de Oliveira, F.P., Oyama, M.D., 2015. Antecedent atmospheric conditions related to squall-line initiation over the northern coast of brazil in july. Weather Forecast. 30 (5), 1254–1264. https://doi.org/10.1175/WAF-D-14-00120.1.

Dias-Júnior, C.Q., Dias, N.L., Fuentes, J.D., Chamecki, M., 2017. Convective storms and non-classical low-level jets during high ozone level episodes in the amazon region: An arm/goamazon case study. Atmos. Environ. 155, 199–209.

Freitas, R.G.E.S., 2006. Estimativa operacional da umidade do solo para iniciação de modelos de previsão numérica da atmosfera parte i: descrição da metodologia e validação. Revista Brasileira de Meteorologia 21 (3), 1–15.

Freitas, S., Longo, K., Silva Dias, M., Chatfield, R., Silva Dias, P., Artaxo, P., Andreae, M., Grell, G., Rodrigues, L., Fazenda, A., Panetta, J., 2009. The coupled aerosol and tracer transport model to the brazilian developments on the regional atmospheric modeling system (catt-brams)–part 1: Model description and evaluation. Atmos. Chem. Phys. 9 (8), 2843–2861.

Freitas, S.R., Longo, K.M., Dias, M.A.S., Dias, P.L.S., Chatfield, R., Prins, E., Artaxo, P., Grell, G.A., Recuero, F.S., 2005. Monitoring the transport of biomass burning emissions in south america. Environ. Fluid Mech. 5 (1–2), 135–167.

Freitas, S.R., Panetta, J., Longo, K.M., Rodrigues, L.F., Moreira, D.S., Rosário, Nilton, E., Dias, Silva, Pedro, L., Maria A F Silva, D., Souza, E.P., Freitas, E.D., Longo, M., Frassoni, A., Fazenda, A.L., Cláudio M Santos, e. S., Pavani, C.A.B., Eiras, D., França, Daniela, A., Massaru, D., Silva, F.B., Santos, F.C., Pereira, G., Camponogara, G., Ferrada, G.A., Velho, Campos, Haroldo, F., Menezes, I., Freire, J.L., Alonso, M.F., Gácita Madeleine, S., Zarzur, M., Fonseca, R.M., Lima, R.S., Siqueira, R.A., Braz, R., Tomita, S., Oliveira, V., Martins, L.D., 2017a. The brazilian developments on the regional atmospheric modeling system (brams 5.2): an integrated environmental model tuned for tropical areas. Geosci. Model Dev. (GMD) 10 (1), 189–222.

Freitas, S.R., Panetta, J., Longo, K.M., Rodrigues, L.F., Moreira, D.S., Rosário, N.E., Silva Dias, P.L., Silva Dias, M.A.F., Souza, E.P., Freitas, E.D., Longo, M., Frassoni, A., Fazenda, A.L., Santos e Silva, C.M., Pavani, C.A.B., Eiras, D., França, D.A., Massaru, D., Silva, F.B., Santos, F.C., Pereira, G., Camponogara, G., Ferrada, G.A., Campos Velho, H.F., Menezes, I., Freire, J.L., Alonso, M.F., Gácita, M.S., Zarzur, M., Fonseca, R.M., Lima, R.S., Siqueira, R.A., Braz, R., Tomita, S., Oliveira, V., Martins, L.D., 2017b. The brazilian developments on the regional atmospheric modeling system (brams 5.2): an integrated environmental model tuned for tropical areas. Geosci. Model Dev. (GMD) 10 (1), 189–222. https://www.geosci-model-dev.net/10/189/2017/.

Fuentes, J.D., Gu, L., Lerdau, M., Atkinson, R., Baldocchi, D., Bottenheim, J., Ciccioli, P., Lamb, B., Geron, C., Guenther, A., Sharkeyj, T., Stockwellk, W., 2000. Biogenic hydrocarbons in the atmospheric boundary layer: a review. Bull. Am. Meteorol. Soc. 81 (7), 1537–1575.

Garstang Jr., M., H. L. M, Halverson, J., Greco, S., Scala, J., 1994. Amazon coastal squall lines. part i: Structure and kinematics. Mon. Weather Rev. 122 (4), 608–622. https://doi.org/10.1175/1520-0493(1994)122<0608:ACSLPI>2.0.CO;2.

Gerken, T., Wei, D., Chase, R.J., Fuentes, J.D., Schumacher, C., Machado, L.A., Andreoli, R.V., Chamecki, M., de Souza, R.A.F., Freire, L.S., Jardine, A.B., Manzi, A.O., dos Santos, R.M.N., von Randow, C., dos Santos Costa, P., Stoy, P.C., Tóta, J., Trowbridge, A.M., 2016. Downward transport of ozone rich air and implications for atmospheric chemistry in the amazon rainforest. Atmos. Environ. 124 (Part A), 64–76.

Grant, D.D., Fuentes, J.D., DeLonge, M.S., Chan, S., Joseph, E., Kucera, P., Ndiaye, S.A., Gaye, A.T., 2008. Ozone transport by mesoscale convective storms in western senegal. Atmos. Environ. 42 (30), 7104–7114.

Grell, G.A., 1993. Prognostic evaluation of assumptions used by cumulus parameterizations. Mon. Weather Rev. 121 (3), 764–787. https://doi.org/10.1175/1520-0493(1993)121<0764:PEOAUB>2.0.CO;2.

Grell, G.A., Dévényi, D., 2002. A generalized approach to parameterizing convection combining ensemble and data assimilation techniques. Geophys. Res. Lett. 29 (14) 38–1-38–4. https://agupubs.onlinelibrary.wiley.com/doi/abs/10.1029/2002GL015311.

Grell, G.A., Freitas, S.R., 2013. A scale and aerosol aware stochastic convective parameterization for weather and air quality modeling. Atmos. Chem. Phys. Discuss. 13 (9).

Grell, G.A., Freitas, S.R., 2014. A scale and aerosol aware stochastic convective parameterization for weather and air quality modeling. Atmos. Chem. Phys. 14 (10), 5233–5250. https://www.atmos-chem-phys.net/14/5233/2014/.

Guenther, A., Karl, T., Harley, P., Wiedinmyer, C., Palmer, P., Geron, C., 2006. Estimates of global terrestrial isoprene emissions using megan (model of emissions of gases and aerosols from nature). Atmos. Chem. Phys. 6 (11), 3181–3210.

Houze Jr., R.A., 1977. Structure and dynamics of a tropical squall-line system. Mon. Weather Rev. 105 (12), 1540–1567. https://doi.org/10.1175/1520-0493(1977)105<1540:SADOAT>2.0.CO;2.

Hu, X.-M., Doughty, D.C., Sanchez, K.J., Joseph, E., Fuentes, J.D., 2012. Ozone variability in the atmospheric boundary layer in maryland and its implications for vertical transport model. Atmos. Environ. 46, 354–364. http://www.sciencedirect.com/science/article/pii/S135223101101017X.

Hu, X.-M., Fuentes, J.D., Zhang, F., 2010. Downward transport and modification of tropospheric ozone through moist convection. J. Atmos. Chem. 65 (1), 13–35.

Hu, X.-M., Klein, P.M., Xue, M., Zhang, F., Doughty, D.C., Forkel, R., Joseph, E., Fuentes, J.D., 2013. Impact of the vertical mixing induced by low-level jets on boundary layer ozone concentration. Atmos. Environ. 70, 123–130. http://www.sciencedirect.com/science/article/pii/S135223101300023X.

Jardine, A., Jardine, K., Fuentes, J., Martin, S., Martins, G., Durgante, F., Carneiro, V., Higuchi, N., Manzi, A., Chambers, J., 2015. Highly reactive light-dependent monoterpenes in the amazon. Geophys. Res. Lett. 42 (5), 1576–1583.

Joyce, R.J., Janowiak, J.E., Arkin, P.A., Xie, P., 2004. Cmorph: A method that produces global precipitation estimates from passive microwave and infrared data at high spatial and temporal resolution. J. Hydrometeorol. 5 (3), 487–503. https://doi.org/10.1175/1525-7541(2004)005<0487:CAMTPG>2.0.CO;2.

Kirchhoff, V.W.J.H., da Silva, I.M.O., Browell, E.V., 1990. Ozone measurements in amazonia: Dry season versus wet season. J. Geophys. Res.: Atmosphere 95 (D10), 16913–16926.

Kousky, V.E., 1980. Diurnal rainfall variation in northeast brazil. Mon. Weather Rev. 108 (4), 488–498.

Machado, L., Laurent, H., Dessay, N., Miranda, I., 2004. Seasonal and diurnal variability of convection over the amazonia: a comparison of different vegetation types and large scale forcing. Theor. Appl. Climatol. 78 (1–3), 61–77.

Martin, S.T., Artaxo, P., Machado, L.A.T., Manzi, A.O., Souza, R.A.F., Schumacher, C., Wang, J., Andreae, M.O., Barbosa, H.M.J., Fan, J., Fisch, G., Goldstein, A.H., Guenther, A., Jimenez, J.L., Pschl, U., Silva Dias, M., Smith, J.N., Wendisch, M., 2016. Introduction: Observations and modeling of the green ocean amazon (goamazon2014/5). Atmos. Chem. Phys. 16 (8), 4785–4797.

Moreira, D.S., Freitas, S.R., Bonatti, J.P., Mercado, L.M., Rosário, N.M.E., Longo, K.M., Miller, J.B., Gloor, M., Gatti, L.V., 2013. Coupling between the jules land-surface scheme and the ccatt-brams atmospheric chemistry model (jules-ccatt-brams1.0): applications to numerical weather forecasting and the co^2 budget in south america. Geosci. Model Dev. (GMD) 6 (4), 1243–1259. https://www.geosci-model-dev.net/6/1243/2013/.

Mota, M., Nobre, C.A., 2006. Relação da variabilidade da energia potential convectiva disponível (cape) com a precipitação e a alta da bolívia durante a campanha wet-amc/lba. Revista Brasileira de Meteorologia 21 (3b), 344–355.

Negrón-Juárez, R.I., Chambers, J.Q., Guimaraes, G., Zeng, H., Raupp, C.F.M., Marra, D.M., Ribeiro, G.H.P.M., Saatchi, S.S., Nelson, B.W., Higuchi, N., 2010. Widespread amazon forest tree mortality from a single cross–basin squall line event. Geophys. Res. Lett. 37 (16). https://agupubs.onlinelibrary.wiley.com/doi/abs/10.1029/2010GL043733.

Negrón-Juárez, R.I., Jenkins, H.S., Raupp, C.F., Riley, W.J., Kueppers, L.M., Magnabosco Marra, D., Ribeiro, G.H., Monteiro, M.T.F., Candido, L.A., Chambers, J.Q., Higuchi, N., 2017. Windthrow variability in central amazonia. Atmosphere 8 (2), 28.

Rosário, N.E., Longo, K.M., Freitas, S.R., Yamasoe, M.A., Fonseca, R.M., 2013. Modeling the south american regional smoke plume: aerosol optical depth variability and surface shortwave flux perturbation. Atmos. Chem. Phys. 13 (6), 2923–2938. https://www.atmos-chem-phys.net/13/2923/2013/.

Rossato, L., Alvalá, R. d. S., Tomasella, J., 2004. Variação espaço-temporal da umidade do solo no brasil: análise das condições médias para o período de 1971-1990. Revista Brasileira de Meteorologia 19 (2), 113–122.

Salmond, J.A., McKendry, I.G., 2005. A review of turbulence in the very stable nocturnal boundary layer and its implications for air quality. Prog. Phys. Geogr.: Earth Environ. 29 (2), 171–188. https://doi.org/10.1191/0309133305pp442ra.

Siqueira, J.R., Machado, L.A.T., 2004. Influence of the frontal systems on the day-to-day convection variability over south america. J. Clim. 17 (9), 1754–1766. https://doi.org/10.1175/1520-0442(2004)017<1754:IOTFSO>2.0.CO;2.

Siqueira, J.R., Rossow, W.B., Machado, L.A.T., Pearl, C., 2005. Structural characteristics of convective systems over south america related to cold-frontal incursions. Mon. Weather Rev. 133 (5), 1045–1064. https://doi.org/10.1175/MWR2888.1.

Sun, J., Burns, S.P., Lenschow, D.H., Banta, R., Newsom, R., Coulter, R., Frasier, S., Ince, T., Nappo, C., Cuxart, J., Blumen, W., Lee, X., Hu, X.-Z., 2002. Intermittent turbulence associated with a density current passage in the stable boundary layer. Boundary-Layer Meteorol. 105 (2), 199–219.

Sun, J., Lenschow, D.H., Burns, S.P., Banta, R.M., Newsom, R.K., Coulter, R., Frasier, S., Ince, T., Nappo, C., Balsley, B.B., Jensen, M., Mahrt, L., Miller, D., Skelly, B., 2004. Atmospheric disturbances that generate intermittent turbulence in nocturnal boundary layers. Boundary-Layer Meteorol. 110 (2), 255–279.

Sun, Z., Shine, K.P., 1994. Studies of the radiative properties of ice and mixed-phase clouds. Q. J. R. Meteorol. Soc. 120 (515), 111–137.

Thompson, G., Eidhammer, T., 2014. A study of aerosol impacts on clouds and precipitation development in a large winter cyclone. J. Atmos. Sci. 71 (10), 3636–3658. https://doi.org/10.1175/JAS-D-13-0305.1.

Thompson, G., Field, P.R., Rasmussen, R.M., Hall, W.D., 2008. Explicit forecasts of winter precipitation using an improved bulk microphysics scheme. part ii: Implementation of a new snow parameterization. Mon. Weather Rev. 136 (12), 5095–5115. https://doi.org/10.1175/2008MWR2387.1.

Toon, O.B., McKay, C., Ackerman, T., Santhanam, K., 1989. Rapid calculation of radiative heating rates and photodissociation rates in inhomogeneous multiple scattering atmospheres. J. Geophys. Res.: Atmosphere 94 (D13), 16287–16301.

Wei, D., Fuentes, J.D., Gerken, T., Chamecki, M., Trowbridge, A.M., Stoy, P.C., Katul, G.G., Fisch, G., Acevedo, O., Manzi, A., von Randow, C., dos Santos, R.M.N., 2018. Environmental and biological controls on seasonal patterns of isoprene above a rain forest in central amazonia. Agric. For. Meteorol. 256–257, 391–406. http://www.sciencedirect.com/science/article/pii/S0168192318301072.

Zipser, E.J., 1977. Mesoscale and convective-scale downdrafts as distinct components of squall-line structure. Mon. Weather Rev. 105 (12), 1568–1589. https://doi.org/10.1175/1520-0493(1977)105<1568:MACDAD>2.0.CO;2.